

Convex Relaxations of Probabilistic AC Optimal Power Flow for Interconnected AC and HVDC Grids

Andreas Venzke, *Student Member, IEEE*, and Spyros Chatzivasileiadis, *Member, IEEE*

Abstract—High Voltage Direct Current (HVDC) lines and grids interconnect AC grids to increase reliability, facilitate integration of electricity markets and connect offshore wind generation. To address the growing uncertainty in the operation of such systems and fully utilize HVDC control capabilities, this work proposes a semidefinite relaxation of a chance constrained AC optimal power flow (OPF) for interconnected AC and HVDC grids, which can achieve zero relaxation gap and provide guarantees for (near-)global optimality. To achieve tractability of the joint chance constraint, a piecewise affine approximation and a combination of randomized and robust optimization is used. We include corrective control policies for HVDC converter active and reactive power, and generator active power and voltage. Using realistic day-ahead forecast data, we demonstrate the performance of our approach on two IEEE 24 bus systems interconnected with an HVDC grid and offshore wind generation, obtaining tight near-global optimality guarantees.

Index Terms—AC optimal power flow, convex optimization, HVDC grids, semidefinite programming, uncertainty.

I. INTRODUCTION

AS consequence of the increase in renewable generation and growing electricity demand, power systems are operated closer to their limits [1]. To maintain a secure operation, significant investment in new transmission capacity and an improved utilization of existing assets are necessary. The High Voltage Direct Current (HVDC) technology is a promising candidate for enabling increased penetration of volatile renewable energy sources and providing controllability in power system operation. In China, in order to transport bulk power, e.g. wind, from geographically remote areas to load centers, significant HVDC transmission capacity has been built [2]. A European HVDC grid is envisioned, extending the several point-to-point connections already in operation to a multi-terminal grid [3]. In this work, we address the challenge of the operation of such a system under uncertainty. To this end, we propose a tractable formulation of the chance constrained AC optimal power flow (OPF) for interconnected AC and HVDC grids which includes HVDC corrective control capabilities.

Several works in the literature integrate models of HVDC grids in the AC-OPF formulation [4], [5]. The work in [4] introduces a generalized steady-state Voltage Source Converter (VSC) multi-terminal DC model which can be used for sequential AC/DC power flow algorithms. The work in [5]

includes security constraints in the AC-OPF formulation for AC grids with HVDC lines to evaluate the potential of post-contingency corrective control with HVDC converters.

To account for uncertainty, chance constraints can be included in the OPF, defining a maximum allowable probability of constraint violation. In literature, the application of chance constraints in the context of interconnected AC and HVDC grids is limited to the DC-OPF formulation [6], [7]. In Ref. [6] a tractable formulation of a probabilistic security constrained DC-OPF is proposed which includes HVDC lines. This framework is extended to include HVDC grids in Ref. [7]. There are two main motivations to use an AC-OPF formulation. First, the DC power flow formulation neglects voltage magnitudes, reactive power and system losses and can lead to substantial errors [8]. Second, the AC-OPF formulation allows to represent and utilize the voltage and reactive power control capabilities of the HVDC converters.

The work in [9] introduces a convex relaxation of the AC-OPF problem for interconnected AC and HVDC grids, using the semidefinite relaxation technique in [10] and including a detailed HVDC converter model. The work in [11] extends this framework towards a security constrained unit commitment problem for AC-DC grids under uncertainty. However, it is assumed that the forecast errors and resulting generation and load mismatch are balanced at each bus internally via curtailment, energy storage or reserve units located at this bus. Hence, the line flows and voltages do not change as a result of different uncertainty realizations. This assumption is restrictive and can lead to high levels of curtailment in practice, e.g. for offshore wind generation without energy storage.

In our previous work [12], we introduced a comprehensive framework to handle chance constraints for the semidefinite relaxation of the AC-OPF, including Gaussian distributions. We further extended this work in [13] by considering security constraints. In this paper, we introduce a tractable formulation of the AC-OPF under uncertainty for interconnected AC and HVDC grids. We model the varying system state due to uncertain power injections, such as varying network flows. The main contributions of our work are:

- To the authors' knowledge, this is the first paper that proposes a convex relaxation of the chance constrained AC-OPF for interconnected AC and HVDC grids.
- Using a piecewise affine approximation of the varying system state, and applying a combination of randomized and robust optimization, we introduce a tractable formulation of the chance constrained AC-OPF for interconnected

A. Venzke and S. Chatzivasileiadis are with the Center for Electric Power and Energy, Technical University of Denmark, Kgs. Lyngby, Denmark. This work is supported by the multiDC project, funded by Innovation Fund Denmark, Grant Agreement No. 6154-00020B.

AC and HVDC grids.

- Our formulation includes piecewise affine corrective control policies for active and reactive power of HVDC converters, generator active power and voltage, and utilizes wind farm reactive power capabilities.
- To allow for scalability of our proposed approach, we decompose the positive semidefinite matrix variables in the semidefinite formulation of the AC-OPF in separate submatrices. Each of these submatrices corresponds to an individual AC or HVDC grid. This also allows an improvement in terms of numerical stability. At the same time, we apply a chordal decomposition of the semidefinite constraints on the submatrices, which further increases the scalability of our approach.
- We investigate the relaxation gap of our solution. By using a penalty term on active power losses, we propose a systematic method to identify suitable penalty weights for zero relaxation gap, i.e. we obtain solutions which are feasible to the original non-convex AC-OPF for interconnected AC and HVDC grids.
- Using realistic day-ahead forecast data, we demonstrate the performance of our approach on two 24 bus systems with an HVDC grid, and two onshore and one offshore wind farm. With a Monte Carlo analysis and using AC-DC power flows of MATACDC [14], we compare our approach to a chance constrained DC-OPF formulation. We find that our approach complies with the considered joint chance constraint whereas the DC-OPF leads to violations. For the considered time steps, the obtained near-global optimality guarantees are higher than 99.5%.

Section II states the semidefinite relaxation of the AC-OPF for interconnected AC and HVDC grids and includes chance constraints. Section III defines the scenario-based uncertainty set, the piecewise affine approximation and formulates corrective control policies. To achieve tractability of the chance constraints, a method from randomized and robust optimization is applied. Section IV presents the results. Section V concludes.

II. AC OPTIMAL POWER FLOW FORMULATION

In this section, we formulate the semidefinite relaxation of the AC-OPF for interconnected AC and HVDC grids and include chance constraints. Ref. [10] proposes a semidefinite relaxation of the AC-OPF by formulating the OPF as a function of a positive semidefinite matrix variable W describing the product of real and imaginary bus voltages. The convex relaxation is obtained by dropping the rank constraint on the matrix W . We build our formulation upon [9], which extends the initial work [10] to AC-DC grids. Among the contributions of this paper is that we decompose the problem, using one matrix W^i for each AC and HVDC grid instead of one matrix W for the entire system, as in [9], and we include a chordal decomposition of the semidefinite constraints on matrices W^i . This allows for scalability and increased numerical stability.

A. Semidefinite Relaxation of AC Optimal Power Flow for Interconnected AC and HVDC Grids

The considered system of interconnected AC and HVDC grids consists of a number of n_{grid} AC and HVDC grids

which are interfaced by a number of n_c HVDC converters. Each HVDC grid is modeled similar to an AC grid, but with purely resistive transmission lines, and generators operating at unity power factor. Each AC and HVDC power grid i is comprised of \mathcal{N}^i buses and \mathcal{L}^i lines. The set of buses with a generator connected is denoted with \mathcal{G}^i . The following auxiliary variables are introduced for each bus $k \in \mathcal{N}^i$ and line $(l, m) \in \mathcal{L}^i$:

$$\begin{aligned} Y_k^i &:= e_k e_k^T Y^i \\ Y_{lm}^i &:= (\bar{y}_{lm}^i + y_{lm}^i) e_l e_l^T - (y_{lm}^i) e_l e_m^T \\ \mathbf{Y}_k^i &:= \frac{1}{2} \begin{bmatrix} \Re\{Y_k^i + (Y_k^i)^T\} & \Im\{(Y_k^i)^T - Y_k^i\} \\ \Im\{Y_k^i - (Y_k^i)^T\} & \Re\{Y_k^i + (Y_k^i)^T\} \end{bmatrix} \\ \mathbf{Y}_{lm}^i &:= \frac{1}{2} \begin{bmatrix} \Re\{Y_{lm}^i + (Y_{lm}^i)^T\} & \Im\{(Y_{lm}^i)^T - Y_{lm}^i\} \\ \Im\{Y_{lm}^i - (Y_{lm}^i)^T\} & \Re\{Y_{lm}^i + (Y_{lm}^i)^T\} \end{bmatrix} \\ \bar{\mathbf{Y}}_k^i &:= \frac{-1}{2} \begin{bmatrix} \Im\{Y_k^i + (Y_k^i)^T\} & \Re\{Y_k^i - (Y_k^i)^T\} \\ \Re\{(Y_k^i)^T - Y_k^i\} & \Im\{Y_k^i + (Y_k^i)^T\} \end{bmatrix} \\ \bar{\mathbf{Y}}_{lm}^i &:= \frac{-1}{2} \begin{bmatrix} \Im\{Y_{lm}^i + (Y_{lm}^i)^T\} & \Re\{Y_{lm}^i - (Y_{lm}^i)^T\} \\ \Re\{(Y_{lm}^i)^T - Y_{lm}^i\} & \Im\{Y_{lm}^i + (Y_{lm}^i)^T\} \end{bmatrix} \\ M_k &:= \begin{bmatrix} e_k e_k^T & 0 \\ 0 & e_k e_k^T \end{bmatrix} \\ M_{lm} &:= \begin{bmatrix} (e_l - e_m)(e_l - e_m)^T & 0 \\ 0 & (e_l - e_m)(e_l - e_m)^T \end{bmatrix} \end{aligned}$$

For each AC and HVDC power grid i , matrix Y^i denotes the bus admittance matrix, e_k the k -th basis vector, \bar{y}_{lm}^i the shunt admittance of line $(l, m) \in \mathcal{L}^i$ and y_{lm}^i the series admittance. The non-linear AC-OPF problem for interconnected AC and HVDC grids can be written as

$$\min_{W^i} \sum_{i=0}^{n_{\text{grid}}} \sum_{k \in \mathcal{G}^i} \{c_{k2}^i (\text{Tr}\{\mathbf{Y}_k^i W^i\} + P_{D_k}^i)^2 + c_{k1}^i (\text{Tr}\{\bar{\mathbf{Y}}_k^i W^i\} + P_{D_k}^i) + c_{k0}^i\} \quad (1)$$

subject to the following constraints for each bus $k \in \mathcal{N}^i$ and line $(l, m) \in \mathcal{L}^i$ of each power grid i :

$$\underline{P}_{G_k}^i \leq \text{Tr}\{\mathbf{Y}_k^i W^i\} + P_{D_k}^i \leq \bar{P}_{G_k}^i \quad (2)$$

$$\underline{Q}_{G_k}^i \leq \text{Tr}\{\bar{\mathbf{Y}}_k^i W^i\} + Q_{D_k}^i \leq \bar{Q}_{G_k}^i \quad (3)$$

$$\underline{V}_k^i \leq \text{Tr}\{M_k^i W^i\} \leq \bar{V}_k^i \quad (4)$$

$$-\bar{P}_{lm}^i \leq \text{Tr}\{\mathbf{Y}_{lm}^i W^i\} \leq \bar{P}_{lm}^i \quad (5)$$

$$\text{Tr}\{\mathbf{Y}_{lm}^i W^i\}^2 + \text{Tr}\{\bar{\mathbf{Y}}_{lm}^i W^i\}^2 \leq \bar{S}_{lm}^i \quad (6)$$

$$W^i = [\Re\{\mathbf{V}^i\} \Im\{\mathbf{V}^i\}]^T [\Re\{\mathbf{V}^i\} \Im\{\mathbf{V}^i\}] \quad (7)$$

The objective (1) minimizes generation cost, where c_{k2}^i , c_{k1}^i and c_{k0}^i are quadratic, linear and constant cost variables associated with power production of generator $k \in \mathcal{G}^i$. The terms $P_{D_k}^i$ and $Q_{D_k}^i$ denote the active and reactive power consumption at bus $k \in \mathcal{N}^i$. Constraints (2) and (3) include the nodal active and reactive power flow balance; $\underline{P}_{G_k}^i$, $\bar{P}_{G_k}^i$, $\underline{Q}_{G_k}^i$ and $\bar{Q}_{G_k}^i$ are generator limits for minimum and maximum active and reactive power, respectively. The bus voltages are constrained by (4) with corresponding lower and upper limits \underline{V}_k^i , \bar{V}_k^i . The active and apparent power branch flow P_{lm}^i and S_{lm}^i on line $(l, m) \in \mathcal{L}^i$ are limited by \bar{P}_{lm}^i (5) and \bar{S}_{lm}^i (6), respectively. The vector of complex bus voltages is denoted

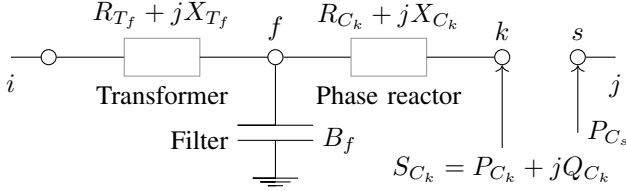


Fig. 1. Model of HVDC VSC connecting AC grid i to HVDC grid j [4].

with \mathbf{V}^i . To obtain an optimization problem linear in W^i , the objective function is reformulated using Schur's complement introducing auxiliary variables α^i :

$$\min_{\alpha^i, W^i} \sum_{i=0}^{n_{\text{grid}}} \sum_{k \in \mathcal{G}^i} \alpha_k^i \quad (8)$$

$$\begin{bmatrix} c_{k1}^i \text{Tr}\{\mathbf{Y}_k^i W^i\} + a_k^i & \sqrt{c_{k2}^i} \text{Tr}\{\mathbf{Y}_k^i W^i\} + b_k^i \\ \sqrt{c_{k2}^i} \text{Tr}\{\mathbf{Y}_k^i W^i\} + b_k^i & -1 \end{bmatrix} \preceq 0 \quad (9)$$

where $a_k^i := -\alpha_k^i + c_{k0}^i + c_{k1}^i P_{D_k}^i$ and $b_k^i := \sqrt{c_{k2}^i} P_{D_k}^i$. In addition, the apparent branch flow constraint (6) is rewritten:

$$\begin{bmatrix} -(\bar{S}_{lm}^i)^2 & \text{Tr}\{\mathbf{Y}_{lm}^i W^i\} & \text{Tr}\{\bar{\mathbf{Y}}_{lm}^i W^i\} \\ \text{Tr}\{\mathbf{Y}_{lm}^i W^i\} & -1 & 0 \\ \text{Tr}\{\bar{\mathbf{Y}}_{lm}^i W^i\} & 0 & -1 \end{bmatrix} \preceq 0 \quad (10)$$

Fig. 1 shows the model of the HVDC converter with filter bus f , AC bus k and DC bus s connecting AC grid i to HVDC grid j . We model the HVDC converters as Voltage Source Converter (VSC) and make the following assumptions [9]: Each VSC can control the active power P_{C_k} , and either the reactive power Q_{C_k} or the AC terminal voltage. A transformer with resistance R_{T_f} and reactance X_{T_f} connects the AC grid to the filter bus f . The resistance R_{C_k} of the phase reactor in the VSC is substantially smaller than its reactance X_{C_k} . The set of converters is denoted with the term \mathcal{C} . The converter is able to modulate the voltage from the AC i to the DC side j by a certain modulation factor m :

$$\frac{\text{Tr}\{\mathbf{M}_k W^i\}}{|V_k|^2} \leq m^2 \frac{\text{Tr}\{\mathbf{M}_s W^j\}}{|V_s^j|^2} \quad (11)$$

The following active power balance has to hold between the AC bus k and DC bus s :

$$P_{C_k} + P_{C_s} + P_{\text{loss},k}^{\text{conv}} = 0 \quad (12)$$

The term $P_{\text{loss},k}^{\text{conv}}$ denotes the converter active power losses. To determine the exact converter losses a detailed assessment of the power electronic switching behavior is necessary, which substantially differs for each converter technology [15]. In this work, we model converter losses as a sum of a constant a_k and a term that depends quadratically with factor c_k on the converter current magnitude $|I_k|$:

$$P_{\text{loss},k}^{\text{conv}} = a_k + c_k |I_k|^2 \quad (13)$$

With Ohm's Law, the current flow magnitude $|I_k|$ from filter bus f to AC bus k of the converter is:

$$|I_k|^2 = (R_{C_k}^2 + X_{C_k}^2)^{-1} \text{Tr}\{\mathbf{M}_{kf} W^i\} \quad (14)$$

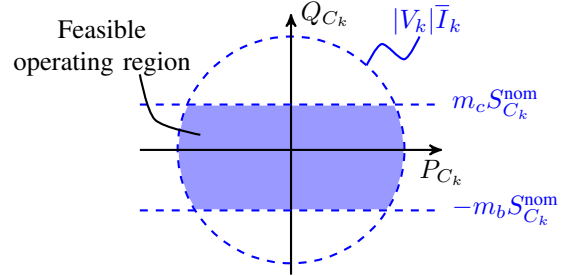


Fig. 2. Active and reactive power capability curve of HVDC converter [16].

The converter current $|I_k|^2$ from (14) can be inserted in the converter power balance (12) using the converter power losses (13) with $z_{C_k} := c_k (R_{C_k}^2 + X_{C_k}^2)^{-1}$:

$$\text{Tr}\{\mathbf{Y}_k W^i\} + \text{Tr}\{\mathbf{Y}_s W^j\} + a_k + z_{C_k} \text{Tr}\{\mathbf{M}_{kf} W^i\} + P_{D_k}^i + P_{D_s}^j = 0 \quad (15)$$

The converter has a feasible operating region to inject and absorb both reactive and active power as depicted in Fig. 2. The maximum reactive power which can be absorbed or injected by the converter is lower- and upper-bounded with positive constants m_b and m_c as follows [16]:

$$-m_b S_{C_k}^{\text{nom}} \leq \text{Tr}\{\bar{\mathbf{Y}}_k W\} \leq m_c S_{C_k}^{\text{nom}} \quad (16)$$

The nominal apparent power rating of the converter is given by $S_{C_k}^{\text{nom}}$. The maximum transferable apparent power S_{C_k} is upper-bounded with the converter current limit \bar{I}_k :

$$|S_{C_k}|^2 = (P_{C_k})^2 + (Q_{C_k})^2 \leq (|V_k| \bar{I}_k)^2 \quad (17)$$

The constraint on the apparent branch flow through the converter (17) is written in matrix form using Schur's complement:

$$\begin{bmatrix} \bar{I}_k^2 \text{Tr}\{\mathbf{M}_k W^i\} & \text{Tr}\{\mathbf{Y}_k^i W^i\} + P_{D_k}^i & \text{Tr}\{\bar{\mathbf{Y}}_k^i W^i\} + Q_{D_k}^i \\ \text{Tr}\{\mathbf{Y}_k^i W^i\} + P_{D_k}^i & 1 & 0 \\ \text{Tr}\{\bar{\mathbf{Y}}_k^i W^i\} + Q_{D_k}^i & 0 & 1 \end{bmatrix} \succeq 0 \quad (18)$$

The non-convex AC-OPF for interconnected AC and HVDC grids minimizes the objective (8) subject to AC and HVDC grid constraints (2) – (5), (7), (9), (10), and HVDC converter constraints (11), (15) – (16), (18). The non-convex rank constraint (7) can be expressed by:

$$W^i \succeq 0 \quad (19)$$

$$\text{rank}(W^i) = 1 \quad (20)$$

The convex relaxation is introduced by dropping the rank constraint (20), relaxing the non-linear, non-convex AC-OPF to a convex semidefinite program (SDP). The work in [10] proves for AC grids that if the rank of W obtained from the SDP relaxation is 1 or 2, then W is the global optimum of the non-linear, non-convex AC-OPF and the optimal voltage vector can be computed following the procedure described in [17]. In [9], there are two necessary conditions to obtain zero relaxation gap for interconnected AC and HVDC grids: First, as in [10], a small resistance of 10^{-4} p.u. has to be included for each transformer. Second, a large resistance of 10^4 p.u. has to be added between the AC bus k and DC bus s of each converter. This is to ensure the resistive connectivity of the

power system graph. In our work, we eliminate the need for the second condition. We formulate the problem not as a function of one matrix W for the whole grid, as in [9], but one matrix W^i for each AC and HVDC grid. This allows us to eliminate the need for the large resistance and still obtain zero relaxation gap. This leads to two desirable effects. First, the numerical stability is increased as the high value of 10^4 p.u. used to be causing numerical scaling problems to the SDP solver in our experiments. Second, the computational run time is reduced, as we consider a reduced amount of matrix entries.

In order to further increase scalability, a chordal decomposition of the semidefinite constraints is applied. Following [18], in order to obtain a chordal graph, a chordal extension of each AC and HVDC grid graph is computed with a Cholesky factorization. Then, we compute the maximum cliques decomposition of the obtained chordal graph. We replace the semidefinite constraint (19) with:

$$(W^i)_{clq,clq} \succeq 0 \quad (21)$$

The positive semidefinite matrix completion theorem ensures that if (21) holds for each maximum clique clq , the resulting matrix W^i can be completed such that it is positive semidefinite. This allows to substantially reduce the number of considered matrix entries and the computational burden [18].

B. Inclusion of Chance Constraints

Renewable energy sources and stochastic loads introduce uncertainty in power system operation. To account for uncertainty in bus power injections, we extend the presented OPF formulation with chance constraints. A total number of n_W wind farms are introduced in the system of interconnected AC and HVDC grids at buses $k \in \mathcal{W}$ and modeled as

$$P_{W_k} = P_{W_k}^f + \zeta_k \quad , \quad (22)$$

where P_W are the actual wind infeeds, $P_{W_k}^f$ are the forecasted values and ζ are the uncertain forecast errors. The convex chance constrained AC-OPF for interconnected AC and HVDC grids includes a joint chance constraint for all buses $k \in \mathcal{N}^i$, lines $(l, m) \in \mathcal{L}^i$ and converters $(s, k, f, i, j) \in \mathcal{C}$:

$$\min_{\alpha^i, W_0^i, W^i(\zeta)} \sum_{i=0}^{n_{\text{grid}}} \sum_{k \in \mathcal{G}^i} \alpha_k^i \quad (23)$$

$$\text{s.t. (9), (2) – (5), (10), (11), (15), (16), (18), (21)}$$

$$\text{for } W^i = W_0^i \quad (24)$$

$$\mathbb{P}\left\{ (2) – (5), (10), (11), (15), (16), (18), (21) \right\} \geq 1 - \epsilon$$

$$\text{for } W^i = W^i(\zeta) \quad (25)$$

For a given maximum allowable violation probability $\epsilon \in (0, 1)$, the joint chance constraint (25) ensures that compliance with the system constraints is achieved with probability higher than the confidence interval $1 - \epsilon$. The system constraints can be classified in two types. The constraints corresponding to equations (2)–(5), (11), (15) – (16) are linear scalar constraints and those corresponding to equations (10), (18), (21) are semidefinite constraints. The matrix W_0^i is the forecasted system

state and the matrix $W^i(\zeta)$ denotes the system state as a function of the forecast errors which are the continuous uncertain variables ζ . Hence, the chance constrained AC-OPF problem (23) – (25) is an infinite-dimensional problem optimizing over $W^i(\zeta)$ [19]. This renders the problem intractable, which makes it necessary to identify a suitable approximation for $W^i(\zeta)$ [20]. In the following, an approximation of an explicit dependence of $W^i(\zeta)$ on the forecast errors is presented.

III. TRACTABLE OPTIMAL POWER FLOW FORMULATION

Using a scenario-based method, we define the uncertainty set associated with forecast errors. As the optimization problem is infinite-dimensional, we use a piecewise affine approximation to model the system state as a function of forecast errors. This allows us to include corrective control policies of active and reactive power set-points of HVDC converters, and of generator active power and voltage set-points. To achieve tractability of the resulting chance constraint, theoretical results from robust optimization are leveraged. By using a penalty term on power losses, we introduce a method to identify suitable penalty terms to achieve zero relaxation gap.

A. Scenario-Based Uncertainty Set

To determine the bounds of the uncertainty set, we use a scenario-based method from [21], which does not make any assumption on the underlying distribution of the forecast errors. To this end, we compute the minimum volume rectangular set which with probability $1 - \beta$ contains $1 - \epsilon$ of the probability mass. The term β is a confidence parameter. According to [19], it is necessary to draw at least the following number of scenarios N_s to specify the uncertainty set:

$$N_s \geq \frac{1}{1 - \epsilon} \frac{e}{e - 1} \left(\ln \frac{1}{\beta} + 2n_W - 1 \right) \quad (26)$$

The term e is Euler's number. The minimum and maximum bounds on the forecast errors ζ are retrieved by a simple sorting operation among the N_s scenarios. The resulting rectangular uncertainty set has a number of n_v vertices $v \in \mathcal{V}$ which are its corner points. For each vertex $v \in \mathcal{V}$, the vector $\bar{\zeta}_v \in \mathbb{R}^{n_W}$ contains the corresponding forecast error magnitudes of the wind farms.

B. Piecewise Affine Approximation

For the previously obtained rectangular uncertainty set, we use the piecewise affine approximation from [12] to model the system change as a function of the forecast errors. To this end, we introduce a matrix W_v^i for each vertex $v \in \mathcal{V}$ and power grid i . The system state of each power grid i as a function of the forecast errors is approximated as a piecewise affine interpolation between the forecasted system state W_0^i and the vertices of the uncertainty set W_v^i :

$$W^i(\zeta) := W_0^i + \Psi_{v=1}^{n_v}(\zeta)(W_v^i - W_0^i)$$

The function $\Psi_{v=1}^{n_v}(\zeta)$ denotes a piecewise affine interpolation operator of the wind forecast error ζ between all vertices $\bar{\zeta}_v$. It returns a weight for the direction of each vertex, corresponding to the distance. For the case of three uncertain wind infeeds, this concept is illustrated in Fig. 3.

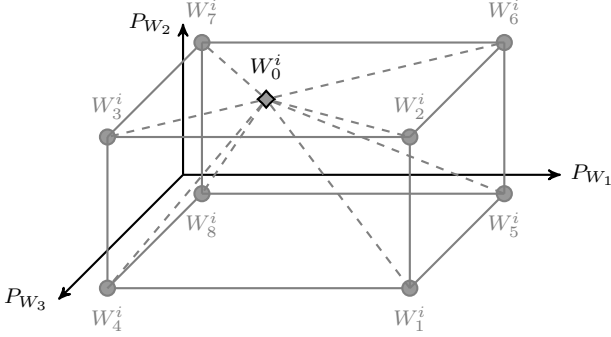


Fig. 3. Uncertainty set derived from the scenario-based method for three wind farms. It is sufficient to enforce the joint chance constraint at the vertices, i.e. at the obtained maximum bounds on forecast errors. For each grid i , the piecewise affine approximation interpolates the system state between the forecasted system states W_0^i and the vertices W_{1-8}^i denoted with circles.

C. Corrective Control Policies

The piecewise affine approximation allows to include corresponding piecewise corrective control policies. We assume that the system operator can respond to forecast errors with corrective control of HVDC converters and generator active power and voltage set-points, i.e. the system operator sends updated set-points based on the realization of forecast errors.

During steady-state power system operation, generation has to match demand and system losses. If an imbalance occurs due to e.g. an occurring forecast error, designated generators in the power grid will respond by adjusting their active power output as part of automatic generation control (AGC). The vector $d_G^i \in \mathbb{R}^{n_b^i}$ defines the generator participation factors for each grid i . The term n_b^i denotes the number of buses of grid i . The vector $d_w^i \in \mathbb{R}^{n_b^i}$ has a $\{-1\}$ entry corresponding to the bus where the w -th wind farm is located. The other entries of this vector are $\{0\}$. The sum of the generator participation factors should compensate the deviation in wind generation, i.e. $\sum_i^{n_{\text{grid}}} \sum_{k \in G} d_{G_k}^i = 1$. The line losses of the AC power grid vary non-linearly with changes in wind infeeds and corresponding adjustments of generator output. To allow for a compensation of the change in system losses, we introduce a slack variable γ_v for each vertex. In order to link the generation dispatch of the forecasted system state W_0^i with system states in which forecast errors occur, the following constraints are introduced for each vertex $v \in \mathcal{V} \setminus \{0\}$, bus $k \in \mathcal{N}^i$ and power grid i :

$$\text{Tr}\{\mathbf{Y}_k^i(W_v^i - W_0^i)\} = \sum_{w=1}^{n_w} \bar{\zeta}_{v,w} (d_{G_k}^i + \gamma_v d_{G_k}^i + d_{w_k}^i) \quad (27)$$

As a result, it is ensured that each generator compensates the non-linear change in system losses proportional to its participation factor. We allow for a corrective control of voltage set-points at generator terminals in case of forecast errors and recover the set-point at bus $k \in \mathcal{N}^i$ and grid i :

$$|\mathbf{V}_k^i|^2 := \text{Tr}\{\mathbf{M}_k W_0^i\} + \Psi_{v=1}^{n_v}(\zeta) \text{Tr}\{\mathbf{M}_k(W_v^i - W_0^i)\}$$

Grid codes specify reactive power capabilities of wind farms often in terms of power factor $\cos \phi = \sqrt{\frac{P^2}{P^2 + Q^2}}$. We allow for a power factor set-point being sent to each wind farm. Note

that our AC-OPF framework captures the variation of the wind farm reactive power injection as a function of wind farm active power. To this end, we modify constraints (3) to include the reactive power capabilities of wind farms. We introduce the reactive power set-point τ_k for each wind farm $k \in \mathcal{W}$:

$$-\sqrt{\frac{1 - \cos^2 \phi}{\cos^2 \phi}} \leq \tau_k \leq \sqrt{\frac{1 - \cos^2 \phi}{\cos^2 \phi}} \quad (28)$$

The HVDC converter can be operated in PV or PQ control mode. Here, we consider the latter, that is the HVDC converter is able to independently control its active and reactive power set-point. Note that our framework can capture the PV control mode as well. The resulting controllability can be utilized to react to uncertain power injections by rerouting active power flows, injecting, or absorbing additional reactive power. In this work, a piecewise affine corrective control policy is introduced for the HVDC converter. The optimization determines an optimal set-point for the active and reactive power of the converter for each vertex and for the operating point. The set-points for a realization of the forecast errors ζ are computed as a piecewise affine interpolation for converter $k \in \mathcal{C}$:

$$\begin{aligned} P_{C_k}(\zeta) &:= \text{Tr}\{\mathbf{Y}_k^i W_0^i\} - P_{D_k}^i + \Psi_{v=1}^{n_v}(\zeta) \text{Tr}\{\mathbf{Y}_k^i(W_v^i - W_0^i)\} \\ Q_{C_k}(\zeta) &:= \text{Tr}\{\bar{\mathbf{Y}}_k^i W_0^i\} - Q_{D_k}^i + \Psi_{v=1}^{n_v}(\zeta) \text{Tr}\{\bar{\mathbf{Y}}_k^i(W_v^i - W_0^i)\} \end{aligned}$$

D. Robust Optimization

To obtain a tractable formulation of the chance constraints including the control policies, the following result from robust optimization is used: If the constraint functions are linear, monotone or convex with respect to the uncertain variables, then the system variables will take the maximum values at the vertices of the uncertainty set [21]. Using the piecewise affine approximation of Section III-B, the system constraints corresponding to equations (2)–(5), (11), (15) – (16) are linear and those corresponding to equations (10), (18), (21) are semidefinite, i.e. convex. Hence, it suffices to enforce the joint chance constraint at the vertices $v \in \mathcal{V}$ of the uncertainty set. We provide a tractable formulation of (25) for each vertex $v \in \mathcal{V}$, bus $k \in \mathcal{N}^i$, line $(l, m) \in \mathcal{L}^i$ and grid i ; the converter constraints are formulated for each converter $(s, k, f, i, j) \in \mathcal{C}$:

$$\underline{P}_k^i \leq \text{Tr}\{\mathbf{Y}_k^i W_v^i\} + P_{D_k}^i - P_{W_k}^f - \bar{\zeta}_{v_k} \leq \bar{P}_k^i \quad (29)$$

$$\underline{Q}_k^i \leq \text{Tr}\{\bar{\mathbf{Y}}_k^i W_v^i\} + Q_{D_k}^i - \tau_k (P_{W_k}^f + \bar{\zeta}_{v_k}) \leq \bar{Q}_k^i \quad (30)$$

$$(\underline{V}_k^i)^2 \leq \text{Tr}\{\mathbf{M}_k W_v^i\} \leq (\bar{V}_k^i)^2 \quad (31)$$

$$-\bar{P}_{lm}^i \leq \text{Tr}\{\mathbf{Y}_{lm}^i W_v^i\} \leq \bar{P}_{lm}^i \quad (32)$$

$$\begin{bmatrix} -(\bar{S}_{lm}^i)^2 & \text{Tr}\{\mathbf{Y}_{lm}^i W_v^i\} & \text{Tr}\{\bar{\mathbf{Y}}_{lm}^i W_v^i\} \\ \text{Tr}\{\mathbf{Y}_{lm}^i W_v^i\} & -1 & 0 \\ \text{Tr}\{\bar{\mathbf{Y}}_{lm}^i W_v^i\} & 0 & -1 \end{bmatrix} \preceq 0 \quad (33)$$

$$W_v^i \succeq 0 \quad (34)$$

$$\text{Tr}\{\mathbf{Y}_k^i(W_v^i - W_0^i)\} = \sum_w^{n_w} \zeta_{v,w} (d_{G_k}^i + \gamma_v d_{G_k}^i + d_{w_k}^i) \quad (35)$$

$$\begin{aligned} \text{Tr}\{\mathbf{Y}_k^i W_v^i\} + \text{Tr}\{\mathbf{Y}_s^i W_v^i\} + a_k + \\ z_{C_k} \text{Tr}\{\mathbf{M}_{kf} W_v^i\} + P_{D_k}^i + P_{D_s}^i = 0 \end{aligned} \quad (36)$$

$$\text{Tr}\{\mathbf{M}_k W_v^i\} \leq m^2 \text{Tr}\{\mathbf{M}_s W_v^j\} \quad (37)$$

$$-m_b S_{C_k}^{\text{nom}} \leq \text{Tr}\{\bar{\mathbf{Y}}_k W_v^i\} \leq m_c S_{C_k}^{\text{nom}} \quad (38)$$

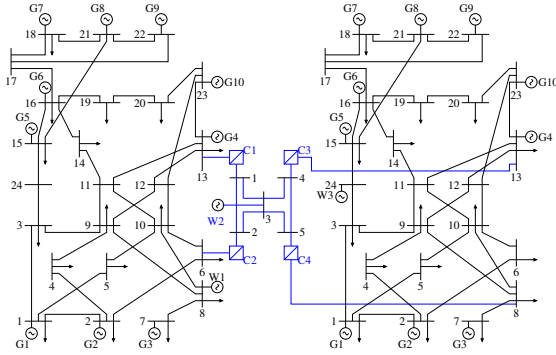


Fig. 4. Two IEEE 24 bus systems interconnected with a 5 bus multi-terminal HVDC grid and two onshore and one offshore wind farm.

$$\begin{bmatrix} \bar{T}_k^2 \text{Tr}\{\mathbf{M}_k W_v^i\} & \text{Tr}\{\mathbf{Y}_k^i W_v\} + P_{D_k}^i & \text{Tr}\{\bar{\mathbf{Y}}_k^i W_v\} + Q_{D_k}^i \\ \text{Tr}\{\mathbf{Y}_k^i W_v^i\} + P_{D_k}^i & 1 & 0 \\ \text{Tr}\{\bar{\mathbf{Y}}_k^i W_v^i\} + Q_{D_k}^i & 0 & 1 \end{bmatrix} \succeq 0 \quad (39)$$

Equation (35) links the forecasted system state with each of the vertices v . The chance constrained AC-OPF formulation minimizes (23) subject to (24), (28), (29) – (39).

E. Systematic Procedure to Obtain Zero Relaxation Gap

With relaxation gap, we refer to the gap between the semidefinite relaxation and a non-linear chance constrained AC-OPF for interconnected AC and HVDC grids which uses the piecewise affine approximation to parametrize the solution space. To obtain zero relaxation gap, a loss penalty term is added to the objective function (23), where the terms $\mu_v \geq 0$ are weighting factors:

$$\min_{\alpha^i, W_0^i, W_v^i, \tau_k, \gamma_v} \sum_{i=0}^{n_{\text{grid}}} \sum_{k \in \mathcal{G}^i} \alpha_k^i + \sum_{v=1}^{n_v} \mu_v \gamma_v \quad (40)$$

We use an individual penalty term μ_v for each vertex and outage instead of a uniform penalty parameter μ as in [12]. We found that this allows us to introduce a robust systematic method to obtain zero relaxation gap, i.e. identify rank-2 solution matrices, as we will show in Section IV. For this purpose, we solve the chance constrained AC-OPF in an iterative manner. First, we set all penalty weights μ_v to 0 and solve the OPF problem. If we obtain rank-2 W solutions, we terminate. Otherwise, we increase the penalty weight μ_v by a defined step-size $\Delta\mu$ only for higher rank matrices and re-solve the OPF problem. We repeat this procedure until all W matrices are rank-2 (in each grid i , there is a W matrix for the operating point, and one additional W matrix for each vertex, see Fig. 3). With this penalized semidefinite AC-OPF formulation, near-global optimality guarantees can be derived, which can specify the maximum distance to the global optimum of a non-convex AC-OPF using the piecewise affine approximation [22]. The numerical results in Section IV show that while this penalty is necessary to obtain zero relaxation gap, in practice the deviation of the near-global optimal solution (40) from the global optimum is small.

IV. SIMULATION AND RESULTS

The optimization problem is implemented in MATLAB using the optimization toolbox YALMIP [23] and the SDP

TABLE I
SIMULATION PARAMETER

Confidence interval $1 - \epsilon$ and parameter β	0.95 10^{-3}	
Wind farm reactive limits on τ ($\cos \phi = 0.95$)	± 0.3827	
HVDC line resistance (p.u.)	0.01	
HVDC upper and lower voltage limits \bar{V}, \underline{V} (p.u.)	1.1 0.9	
Converter apparent power S_C^{nom} (MVA)	200	
Converter voltage rating (kV)	240	
Resistance R_{T_k} , reactance X_{T_k} (p.u.) [4]	0.0015	0.1121
Converter resistance R_{C_k} , reactance X_{C_k} (p.u.) [4]	0.0001	0.1643
Converter loss terms a_k, c_k (p.u.) [4]	0.0110	0.0069
Filter B_f (multi-modular converter has no filter)	–	
Upper converter current limit	$\frac{1}{1.1} \cdot S_C^{\text{nom}}$	
Voltage modulation m	1.05	
Upper and lower converter reactive limits m_c, m_b	0.4 0.5	

solver MOSEK 8 [24]. A small resistance of 10^{-4} p.u. has to be added to each transformer, which is a condition for obtaining zero relaxation gap [10]. To investigate whether the relaxation gap of an obtained solution matrix W^i is zero, the ratio ρ of the 2nd to 3rd eigenvalue of each maximum clique clq is computed, a measure proposed by [17]. This value should be around 10^5 or larger for zero relaxation gap to hold and implies that the obtained solution matrix is rank-2. The respective rank-1 solution can be retrieved by following the procedure in [17]. The obtained solution is then a feasible solution to the original non-linear AC-OPF. The work in [22] proposes the use of the following measure to evaluate the degree of the near-global optimality of a penalized relaxation: Let $\tilde{f}_1(x)$ be the generation cost of the convex OPF without a penalty term and $\tilde{f}_2(x)$ the generation cost with a penalty weight sufficiently high to obtain rank-2 matrices. The near-global optimality can be assessed by computing the parameter $\delta_{\text{opt}} := \frac{\tilde{f}_1(x)}{\tilde{f}_2(x)} \cdot 100\%$. Note that this distance is an upper bound to the distance from the global optimum. For the following analysis, we consider a 53-bus system, i.e. two IEEE 24 bus systems interconnected with a 5 bus HVDC grid shown in Fig. 4. A total of three on- and offshore wind farms with a rated power of 150 MW, 300 MW and 400 MW are placed at bus 8 of the first AC grid, at bus 24 of the second AC grid, and at bus 3 of the HVDC grid, respectively. Table I shows the simulation parameters. For the generator participation factors, each generator adjusts its active power proportional to its maximum active power.

A. Systematic Procedure to Obtain Zero Relaxation Gap

In this section, we showcase the systematic procedure to obtain zero relaxation gap, i.e. to identify rank-2 solution matrices. For illustrative purposes, we assume for each wind farm a forecasted infeed of 50% of rated power and assume the forecast error bounds are within $\pm 25\%$ of rated power with 95% probability. We select the penalty weight step size $\Delta\mu$ to be 25. In Fig. 5, we show minimum eigenvalue ratios ρ of all grids i , generation cost and penalty for each iteration of the proposed systematic procedure. At iteration 25 we obtain zero relaxation gap, i.e. matrices W_{0-8}^i are rank-2. At this point, the near-global optimality guarantee evaluates to 99.52%, i.e. the distance to the global optimum is at most 0.48%. The

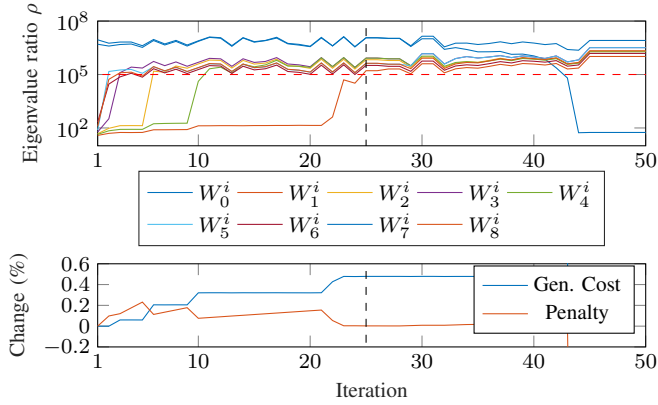


Fig. 5. Minimum eigenvalue ratios ρ of all grids i , generation cost and penalty for each iteration of the systematic procedure for the considered test case. The change of generation cost and penalty is normalized to the non-penalized objective value. The procedure would terminate at iteration 25. In this test case only, we extend the number of iterations to 50 to further investigate the relationship between eigenvalue ratio and penalty parameter. For this purpose, once we reach the defined minimum clique eigenvalue ratio, we double it.

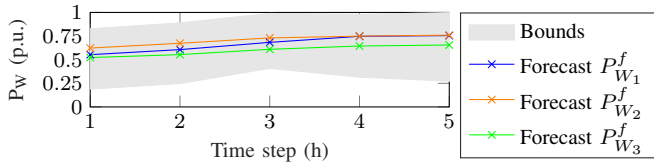


Fig. 6. Wind forecast from hour 1 to hour 7: The bounds correspond to the overall minimum and maximum value of the individual bounds of each forecast error for the N_s sampled scenarios. In the optimization we do consider though the individual bounds for each wind farm.

proposed procedure allows for a systematic identification of suitable penalty weights. This improves upon previous works [12], [25] which use an ad-hoc defined penalty parameter. In case simulations with similar setup are rerun, the previously obtained penalty weights μ_v can be used as hot start.

B. Monte Carlo Analysis Using Realistic Forecast Data

In this section, we compare the proposed chance constrained AC-OPF to a DC-OPF formulation [7] and to an AC-OPF without considering uncertainty, for the test case shown in Fig. 4 using realistic forecast data. Note that in literature the application of chance constraints to interconnected AC and HVDC grids is limited to the DC-OPF formulation. We select the penalty weight step size $\Delta\mu$ to be 100. The DC-OPF includes a joint chance constraint on active generator power and active line flows, and corrective control of active power set-points of HVDC converters. As the branch flow limits are specified in terms of apparent power, for the DC-OPF only we set the maximum active branch flow to 80% \bar{S}_{lm} . To construct the rectangular uncertainty set for both formulations, we draw $N_S = 377$ samples from realistic day-ahead wind forecast scenarios from [26]. The forecasts are based on wind power measurements in the Western Denmark area from 15 different control zones collected by the Danish transmission system operator Energinet. We select control zone 1, 11, 3 to correspond to the wind farm at bus 8, 24, and 3, respectively. The forecast data and forecast error bounds for the 5 considered time steps are shown in Fig. 6. The converter C2 is selected

TABLE II
COMPARISON OF PERFORMANCE OF AC-OPF WITHOUT CONSIDERING UNCERTAINTY, THE CHANCE-CONSTRAINED AC-OPF FORMULATION AND A CHANCE-CONSTRAINED DC-OPF [7] USING 10'000 SAMPLES FROM REALISTIC FORECAST DATA. INSECURE INSTANCES ARE MARKED BOLD.

Time step (h)	1	2	3	4	5
Empirical bus voltage constraint violation probability (%)					
AC-OPF w/o CC	24.07	24.24	15.71	13.85	23.35
CC-AC-OPF	0.0	0.0	0.0	0.0	0.0
CC-DC-OPF [7]	100.0	100.0	100.0	100.0	100.0
Empirical generator active power constraint violation probability (%)					
AC-OPF w/o CC	100.0	100.0	100.0	100.0	100.0
CC-AC-OPF	0.0	0.0	0.0	0.0	0.0
CC-DC-OPF [7]	9.50	2.31	11.58	1.10	0.73
Empirical apparent branch flow constraint violation probability (%)					
AC-OPF w/o CC	0.0	0.0	0.0	0.0	0.0
CC-AC-OPF	0.0	0.0	0.0	0.0	0.0
CC-DC-OPF [7]	0.0	0.0	0.0	0.0	0.0
Cost of uncertainty (%)					
CC-AC-OPF	3.94	4.78	3.95	5.07	5.54
CC-DC-OPF [7]	1.42	2.25	1.85	3.16	3.69
Near-global optimality guarantee δ_{opt} (%)					
CC-AC-OPF	99.63	99.60	99.53	99.65	99.58

as DC slack bus which compensates the possible mismatch between set-points and the realized active power flows. Note that the DC-OPF approach does not model converter losses and that the AC-OPF without considering uncertainty includes no corrective control policies, i.e. resulting mismatches are compensated via the slack bus converter. With our approach we include suitable HVDC converter corrective control policies.

In order to evaluate the empirical constraint violation probabilities of the three approaches, we run a Monte Carlo analysis using AC-DC power flows of MATA CDC [14] with 10'000 samples drawn from the realistic forecast data. MATA CDC is a sequential AC/DC power flow solver interfaced with MATPOWER [27] which uses the HVDC converter model shown in Section II-A. The DC-OPF provides only the active power set-points for generators and HVDC converters. To exclude numerical errors, a minimum violation limit of 10^{-3} per unit for generator limits on active power and 0.1% for voltage and apparent line flow limits is assumed. In the AC power flow the generator reactive power limits are enforced to avoid a possibly high non-physical overloading of the limits. Furthermore, we distribute the loss mismatch from the active generator set-points among the generators according to their participation factors and rerun the power flow to mimic the response of automatic generation control (AGC).

In Table II the resulting violation probability of the joint chance constraint on active power, bus voltages, and active branch flows, and the cost of uncertainty are compared for our approach, an AC-OPF without considering uncertainty and the chance constrained DC-OPF. We find that our proposed

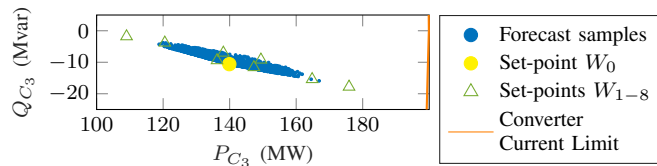


Fig. 7. Corrective control policy of converter active and reactive power set-points and 10'000 sample realizations for converter C3 and time step 3.

approach complies with the joint chance constraint. If we do not consider uncertainty in the AC-OPF, violations of generator and voltage limits occur. The chance constrained DC-OPF violates the target value of $\epsilon = 5\%$ as well. Violations of voltage limits occur as the DC-OPF approximation does not model voltage magnitudes. As losses which can make up several percent of load are also neglected, the limits on generator active power are violated as well. The cost of uncertainty is lower for the DC-OPF approach as the cost for the active power losses are not included. On average, for our approach, the total solving time is 13.0 seconds, the individual SDP solving time is 1.9 seconds and the number of iterations for the systematic procedure to obtain zero relaxation gap is 6.8. For all considered time steps, the near-global optimality guarantee evaluates to at least 99.5%. For the HVDC converter C3 and time step 3, we show in Fig. 7 the active and reactive power set-points from our approach and the resulting 10'000 realizations which comply with the HVDC converter limits.

V. CONCLUSIONS

In this work, we propose a semidefinite relaxation of a chance constrained AC-OPF for interconnected AC and HVDC grids, which can achieve zero relaxation gap and guarantee (near-)global optimality. We include control policies related to active power, reactive power, and voltage, in particular of HVDC converters. To enhance scalability and numerical stability, we split the semidefinite matrix in parts corresponding to each individual subsystem, i.e. different AC or DC grids, and apply a chordal decomposition. By using a penalty term on active power losses, we propose systematic method to identify suitable penalty weights for zero relaxation gap. For a test case of two IEEE 24 bus AC grids interconnected through an HVDC grid, using realistic forecast data, we show that a chance constrained DC-OPF leads to violations of the considered joint chance constraint whereas our proposed approach achieves compliance. Notably, our approach obtains tight near-global optimality guarantees specifying the distance to the global optimum to be upper bounded by $\leq 1\%$ of the objective value. Our future work will focus on (i) N-1 security constraints and (ii) Gaussian distributions.

REFERENCES

- [1] T. Brown, P.-P. Schierhorn, E. Tröster, and T. Ackermann, "Optimising the European transmission system for 77% renewable electricity by 2030," *IET Renewable Power Generation*, vol. 10, no. 1, pp. 3–9, 2016.
- [2] D. Bogdanov and C. Breyer, "North-East Asian Super Grid for 100% renewable energy supply: Optimal mix of energy technologies for electricity, gas and heat supply options," *Energy Conversion and Management*, vol. 112, pp. 176–190, 2016.
- [3] E. Pierri, O. Binder, N. G. Hemdan, and M. Kurrat, "Challenges and opportunities for a European HVDC grid," *Renewable and Sustainable Energy Reviews*, vol. 70, pp. 427–456, 2017.

- [4] J. Beerten, S. Cole, and R. Belmans, "Generalized steady-state VSC MTDC model for sequential AC/DC power flow algorithms," *IEEE Transactions on Power Systems*, vol. 27, no. 2, pp. 821–829, 2012.
- [5] S. Chatzivasileiadis and G. Andersson, "Security constrained OPF incorporating corrective control of HVDC," in *Power Systems Computation Conference (PSCC)*, 2014.
- [6] M. Vrakopoulou, S. Chatzivasileiadis, and G. Andersson, "Probabilistic security-constrained optimal power flow including the controllability of HVDC lines," in *IEEE PES ISGT Europe*, 2013.
- [7] R. Wiget, M. Vrakopoulou, and G. Andersson, "Probabilistic security constrained optimal power flow for a mixed HVAC and HVDC grid with stochastic infeed," in *Power Systems Computation Conference (PSCC)*, 2014.
- [8] K. Dvijotham and D. Molzahn, "Error Bounds on the DC Power Flow Approximations: A Convex Relaxation Approach," *IEEE 55th Conference on Decision and Control (CDC)*, December 2016.
- [9] S. Bahrami, F. Therrien, V. W. Wong, and J. Jatskevich, "Semidefinite relaxation of optimal power flow for AC-DC grids," *IEEE Transactions on Power Systems*, vol. 32, no. 1, pp. 289–304, 2017.
- [10] J. Lavaei and S. H. Low, "Zero duality gap in optimal power flow problem," *IEEE Transactions on Power Systems*, vol. 27, no. 1, pp. 92–107, 2012.
- [11] S. Bahrami and V. W. S. Wong, "Security-constrained unit commitment for ac-dc grids with generation and load uncertainty," *IEEE Transactions on Power Systems*, vol. PP, no. 99, pp. 1–1, 2017.
- [12] A. Venzke, L. Halilbasic, U. Markovic, G. Hug, and S. Chatzivasileiadis, "Convex relaxations of chance constrained AC optimal power flow," *IEEE Transactions on Power Systems*, vol. PP, no. 99, pp. 1–1, 2017.
- [13] A. Venzke and S. Chatzivasileiadis, "Convex relaxations of security constrained AC optimal power flow under uncertainty," in *Power Systems Computation Conference (PSCC), Dublin*, 2018.
- [14] J. Beerten and R. Belmans, "Development of an open source power flow software for high voltage direct current grids and hybrid AC/DC systems: MATAADC," *IET Generation, Transmission & Distribution*, vol. 9, no. 10, pp. 966–974, 2015.
- [15] P. S. Jones and C. C. Davidson, "Calculation of power losses for MMC-based VSC HVDC stations," in *15th European Conference on Power Electronics and Applications (EPE)*, 2013.
- [16] M. C. Imhof, "Voltage Source Converter based HVDC-modelling and coordinated control to enhance power system stability," Ph.D. dissertation, ETH Zurich, 2015.
- [17] D. K. Molzahn, J. T. Holzer, B. C. Lesieutre, and C. L. DeMarco, "Implementation of a large-scale optimal power flow solver based on semidefinite programming," *IEEE Transactions on Power Systems*, vol. 28, no. 4, pp. 3987–3998, 2013.
- [18] R. A. Jabr, "Exploiting sparsity in SDP relaxations of the OPF problem," *IEEE Transactions on Power Systems*, vol. 27, no. 2, pp. 1138–1139, 2012.
- [19] M. Vrakopoulou, M. Katsampani, K. Margellos, J. Lygeros, and G. Andersson, "Probabilistic security-constrained AC optimal power flow," in *IEEE PowerTech (POWERTECH)*, Grenoble, France, 2012.
- [20] A. Ben-Tal and A. Nemirovski, "Selected topics in robust convex optimization," *Mathematical Programming*, vol. 112, no. 1, pp. 125–158, 2008.
- [21] K. Margellos, P. Goulart, and J. Lygeros, "On the road between robust optimization and the scenario approach for chance constrained optimization problems," *IEEE Transactions on Automatic Control*, vol. 59, no. 8, pp. 2258–2263, 2014.
- [22] R. Madani, S. Sojoudi, and J. Lavaei, "Convex relaxation for optimal power flow problem: Mesh networks," *IEEE Transactions on Power Systems*, vol. 30, no. 1, pp. 199–211, 2015.
- [23] J. Löfberg, "YALMIP : A toolbox for modeling and optimization in MATLAB," in *In Proceedings of the CACSD Conference*, Taipei, Taiwan, 2004.
- [24] MOSEK ApS, *MOSEK 8.0.0.37*, 2016.
- [25] R. Madani, M. Ashraphijuo, and J. Lavaei, "Promises of conic relaxation for contingency-constrained optimal power flow problem," *IEEE Transactions on Power Systems*, vol. 31, no. 2, pp. 1297–1307, 2016.
- [26] W. A. Bukhsh, C. Zhang, and P. Pinson, "An integrated multiperiod OPF model with demand response and renewable generation uncertainty," *IEEE Transactions on Smart Grid*, vol. 7, no. 3, pp. 1495–1503, 2016.
- [27] R. D. Zimmerman, C. E. Murillo-Sánchez, and R. J. Thomas, "MATPOWER: Steady-state operations, planning, and analysis tools for power systems research and education," *IEEE Transactions on Power Systems*, vol. 26, no. 1, pp. 12–19, 2011.